Research Article GU J Sci 35(1): 148-165 (2022) DOI: 10.35378/gujs.860783

Gazi University

Journal of Science

http://dergipark.gov.tr/gujs

Analytical Modeling of Buckling Behavior of Porous FGM Cylindrical Shell Embedded within an Elastic Foundation

Abdelaziz TIMESLI*

Hassan II University of Casablanca, National Higher School of Arts and Crafts of Casablanca, SEISEE Laboratory, 20670, Casablanca, Morocco

Highlights

- We develop analytical models to analyze the buckling behavior of embedded porous FGM shell.
- The modified rule of mixture is used to implement the behavior of porous FGM cylindrical shell.
- The proposed formulas can be used to study the influences of several parameters of porous FGM Shell.

Article Info

Received: 14 Jan 2021
Accepted:13 Mar 2021

Keywords

Stability analysis
Porous FGM shell
Elastic foundation
Cylindrical shell theory

Abstract

The aim of this paper is to investigate the buckling behavior of porous Functionally Graded Materiel (FGM) cylindrical shells based on Donnell shell theory. In this context, we develop an explicit analytical expression which takes into consideration the effect of porosities through the thickness of the structure and that of the elastic foundation using a modified power-law function and the models of Winkler and Pasternak, respectively. We use the modified rule of mixture to determinate the behavior of the porous FGM cylindrical shell. The effects of porosity volume fraction, power-law index, and Young's modulus ratio are investigated. Moreover, we also discuss the influence of different parameters on the stability behavior of the porous FGM shell.

1. INTRODUCTION

In materials science, among the most impressive discoveries are FGMs. The use of this kind of materials is dramatically increasing in several engineering structures (e.g., mechanics, civil engineering, aerospace, and nuclear) [1], what has prompted many scientists in recent years to expect the mechanical behavior of such structures [2-10]. FGMs are considered as advanced composite materials constituted of at least two different materials, the first one resists high temperatures as the ceramic and the second one with high mechanical rigidity as the metal [11]. In this kind of material, the variation of the properties over volume is continuous to avoid certain problems, as an example stress concentrations and delamination, encountered by the traditional composites which encounter many problems because of the existence an interface between metals and ceramics. Properties of FGMs can be affected considerably by the existence of porosities, therefore it is important to consider the effect of porosity for a more efficient manufacturing of FGMs and their technical design [12-16]. Porous FGMs [17-19] combine both FG characteristics and porosity and can be designed by producing porosities inside FGMs using the fabrication processes based on different technical issues. The porosity can evolve gradually through volume providing desirable properties for some areas of engineering such as the biomedical, and undesirable properties for other areas such as the aeronautical sector. Moreover, the porosity can be changed in one or more directions using the pore size alteration or the local density effects. Functionally Graded Porous (FGP) materials have a classified cell-based structure, this classification can be closed or open. The most concerned structures for the analysis of porous materials behaviors are the beams, plates and shells. Several beam theories have been developed to study the response of porous materials under external loads and different types of boundary conditions, as examples Ebrahimi et al. (2015) [20] analyzed the nonlinear vibration of porous FGM beams, Chen et al. (2016) [21] examined the shear deformable sandwich beam made of FGP core, they are interested in this

* e-mail: ABDELAZIZ.TIMESLI@univh2c.ma, abdelaziz.timesli@gmail.com

study by the nonlinear free vibration of this kind of material, Atmane et al. (2017) [22] analyzed the mechanical response of a porous FGM beams embedded on elastic foundations, they investigate the effect of both thickness stretching and porosity and Berghouti et al. (2019) [23] presented the dynamic response of porous FGM nano-beams. Now we present some research works based on plates theories to model porous materials, Medani et al. (2019) [24] examined the behavior of porous plates made of sandwich polymer and reinforced by functionally graded carbon nanotubes, Kaddari et al. (2020) [25] developed a new theory based on quasi-3D hyperbolic shear deformation to discuss the statics and free vibration of FGP plates embedded in Kerr-type elastic foundation, Jena et al. (2020) [26] used Navier's technique and shifted Chebyshev polynomial-based Rayleigh-Ritz method to study the vibration of a FGP beam resting on Kerr foundation and Tran et al. (2020) [27] analyzed a free vibration of the FGP plates embedded in an elastic foundation. The use of shell theories to model porous materials is not used much in the literature, Ebrahimi et al. (2019) [28] used an analytical method to analyze the vibration of an embedded cylindrical shell made of porous metal foam, they studied the influence of different models of porosity distribution, Jouneghani et al. (2017) [29] analyzed the free vibration of porous FGM doubly-curved shells using the first-order shear deformation theory, Wang et al. (2018) [30] identified the effect of temperature and that of porosities on the vibrations of FG cylindrical shells and Keddouri et al. (2019) [31] introduced a new displacement based high-order shear deformation theory to study the static behavior of FG sandwich plate taking into account a new expression of porosity distribution. For researchers in the literature, the theoretical researches on dynamic and stability of porous FGM beams, plates or shells are very interesting.

We choose in this work to use the cylindrical shell theory based on Donnell shell theory [32-36] to describe mechanical behavior of porous FGM cylindrical shells. In this theory of circular cylindrical shells, the median surface of the shell and the thin shell assumption in the derivation, respectively, are used to calculate the induced stresses and to neglect the transverse-shear and rotary-inertia effects. This theory is based on the simplifying shallow-shell hypothesis where it has been widely used because it is practically accurate and relatively simple. The introduction of a stress function is the most used form of Donnell shell theory, the objective is to combine the three equations of equilibrium representing the shell displacements in the radial, circumferential and axial directions, which makes it possible to reduce the equilibrium in two equations as a function of the radial displacement w and the stress function. This theory gives accurate results if we take into consideration the following hypotheses: large aspect ratio ($radius/length \geq 10$), $(thickness/radius)^2 \ll 1$ and $(1/n)^2 \ll 1$ where n is the circumferential half wavenumber.

Buckling phenomenon can be studied analytically, numerically and experimentally [33-35, 37, 38]. The objective of this research is to purpose an analytical expression to study the buckling behavior of porous FGM cylindrical shell embedded in an elastic foundation. This expression is obtained using a continuum approach which is developed using the assumptions of Donnell's cylindrical shell theory. We depend on the analytical minimization to derive the critical buckling load. The elastic foundation is modeled with Winkler and Pasternak models. We discuss the effects of power-law index, porosity volume fraction, Young's modulus ratio, and elastic foundation parameters. Compared to the existing literature for buckling behavior of porous FGM cylindrical shell resting on an elastic foundation, the developments of this paper is the use of analytical modeling and Kerr foundation.

2. GOVERNING EQUATIONS OF POROUS FGM CYLINDRICAL SHELL

We consider that the porous FGM cylindrical shell as a circular cylindrical thin-walled shell of radius R, wall thickness h which is much lower than R, and length L (see Figure 1-(a)). Young's modulus E and Poisson's ratio υ of porous FGM shell are computed according to the modified rule of mixture [30]. The porous FGM shell is embedded in elastic foundation as shown in Figure 1-(b), which allows us to examine the effect of different parameters of the elastic foundation on the buckling behavior. These parameters are the lower spring modulus K_W called also Winkler modulus, the shear layer modulus K_G and the upper spring modulus K_C.

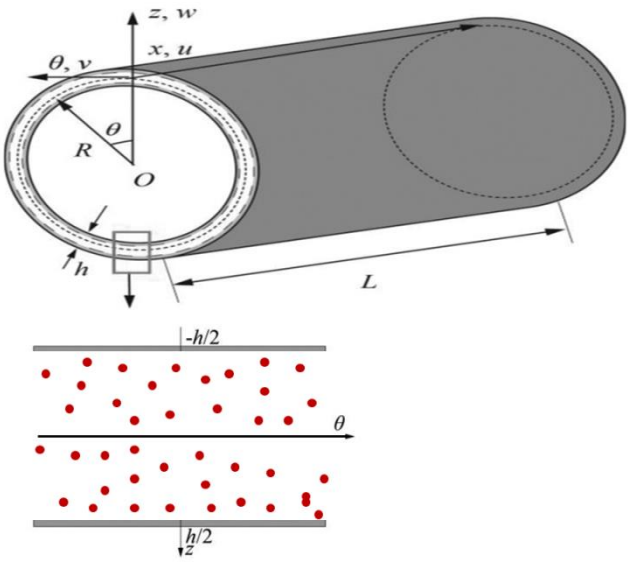

(a): Thin-walled circular cylindrical shell

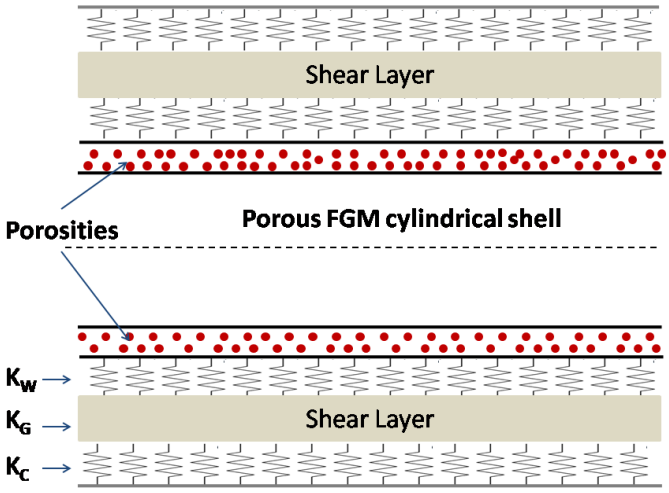

(b): Porous FGM cylindrical shell resting on the Kerr foundation

Figure 1. *Porous FGM cylindrical shell resting on the elastic foundation*

The equilibrium equation the thin-walled circular cylindrical shell is based Donnell model and it can be written as [33-35]:

$$\frac{\partial^2 M_{xx}}{\partial x^2} + \frac{2}{R}\frac{\partial^2 M_{x\theta}}{\partial x \partial \theta} + \frac{1}{R^2}\frac{\partial^2 M_{\theta\theta}}{\partial \theta^2} + \frac{N_{\theta\theta}}{R} + N_{xx}\frac{\partial^2 w}{\partial x^2} + \frac{2N_{x\theta}}{R}\frac{\partial^2 w}{\partial x \partial \theta} + \frac{N_{\theta\theta}}{R^2}\frac{\partial^2 w}{\partial \theta^2} - f, \tag{1}$$

where N_{xx} and $N_{\theta\theta}$ are normal forces, $N_{x\theta}$ is the internal shear force, M_{xx} and $M_{\theta\theta}$ are bending moments and $M_{x\theta}$ is the twisting moment, w is the displacement of the reference surface and f external load which is related to the elastic foundation model. M_{xx}, $M_{\theta\theta}$ and $M_{x\theta}$ are given as follows:

$$\begin{cases} M_{xx} = -D_{11}\dfrac{\partial^2 w}{\partial x^2} - \dfrac{D_{12}}{R^2}\dfrac{\partial^2 w}{\partial \theta^2} \\ M_{\theta\theta} = -D_{12}\dfrac{\partial^2 w}{\partial x^2} - \dfrac{D_{22}}{R^2}\dfrac{\partial^2 w}{\partial \theta^2}, \\ M_{x\theta} = -2\dfrac{D_{66}}{R}\dfrac{\partial^2 w}{\partial x \partial \theta} \end{cases} \tag{2}$$

where D_{ij} are the bending stiffness coefficients of the shell, they are given by:

$$\begin{cases} D_{11} = D_{22} = \int_{-h/2}^{h/2} \left(z^2 \frac{E(z)}{(1-\nu(z)^2)} \right) dz \\ D_{12} = \int_{-h/2}^{h/2} \left(z^2 \frac{\nu(z)E(z)}{(1-\nu(z)^2)} \right) dz \\ D_{66} = \int_{-h/2}^{h/2} \left(z^2 \frac{E(z)}{2(1+\nu(z))} \right) dz \end{cases} . \tag{3}$$

Replacing the bending stiffness coefficients in Equation (1) and we obtain:

$$-D\left(\frac{\partial^4 w}{\partial x^4} + \frac{2}{R^2}\frac{\partial^4 w}{\partial x^2 \partial \theta^2} + \frac{1}{R^4}\frac{\partial^4 w}{\partial \theta^4}\right) + \frac{N_{\theta\theta}}{R} + N_{xx}\frac{\partial^2 w}{\partial x^2} + \frac{2N_{x\theta}}{R}\frac{\partial^2 w}{\partial x \partial \theta} + \frac{N_{\theta\theta}}{R^2}\frac{\partial^2 w}{\partial \theta^2} - f, \tag{4}$$

where $D = D_{11} = D_{22} = D_{12} + 2D_{66}$. In the Donnell shell theory, the membrane forces can be connected to the stress function ϕ and we can write them as follows $N_{xx} = \frac{1}{R^2}\frac{\partial^2 \phi}{\partial \theta^2}$, $N_{\theta\theta} = \frac{\partial^2 \phi}{\partial x^2}$ and $N_{x\theta} = \frac{1}{R}\frac{\partial^2 \phi}{\partial x \partial \theta}$. The study of different possible equilibrium configurations is based on the adjacent equilibrium criterion [33-35]. For that the indices 0 and b represent, respectively, pre-buckling and post-buckling quantities and the terms of second order in index b are neglected, we can therefore show the equilibrium equation as follows:

$$-D\left(\frac{\partial^4 w_b}{\partial x^4} + \frac{2}{R^2}\frac{\partial^4 w_b}{\partial x^2 \partial \theta^2} + \frac{1}{R^4}\frac{\partial^4 w_b}{\partial \theta^4}\right) + \frac{1}{R}\frac{\partial^2 \phi}{\partial x^2} + N_{xx0}\frac{\partial^2 w_b}{\partial x^2} + \frac{2N_{x\theta 0}}{R}\frac{\partial^2 w_b}{\partial x \partial \theta} + \frac{N_{\theta\theta 0}}{R^2}\frac{\partial^2 w_b}{\partial \theta^2} - f_b = 0. \tag{5}$$

The compatibility condition of the stress function $\phi(x,\theta)$ is given by:

where

$$\begin{cases} C_{11}^* = C_{22}^* = \dfrac{C_{11}}{\Delta} = \dfrac{C_{22}}{\Delta} \\ C_{12}^* = -\dfrac{C_{12}}{\Delta} \\ C_{66}^* = \dfrac{1}{C_{66}} \end{cases} \tag{7}$$

where C_{ij} are the extensional stiffness coefficients of the shell which are given by:

$$\begin{cases} C_{11} = C_{22} = \int_{-h/2}^{h/2} \left(\frac{E(z)}{(1-\nu(z)^2)} \right) dz \\ C_{12} = \int_{-h/2}^{h/2} \left(\frac{\nu(z)E(z)}{(1-\nu(z)^2)} \right) dz \\ C_{66} = \int_{-h/2}^{h/2} \left(\frac{E(z)}{2(1+\nu(z))} \right) dz \end{cases} , \tag{8}$$

with

$$\Delta = C_{11}^2 = C_{12}^2. \tag{9}$$

The shear membrane forces, the axial compression and the circumferential membrane force are, respectively, given by $N_{x\theta 0} = 0$, $N_{xx0} = P$, and $N_{\theta\theta 0} = 0$, then the system (5)-(6) becomes:

$$\begin{cases} -D\left(\dfrac{\partial^4 w_b}{\partial x^4} + \dfrac{2}{R^2}\dfrac{\partial^4 w_b}{\partial x^2 \partial \theta^2} + \dfrac{1}{R^4}\dfrac{\partial^4 w_b}{\partial \theta^4}\right) + \dfrac{1}{R}\dfrac{\partial^2 \phi}{\partial x^2} + \lambda\dfrac{\partial^2 w_b}{\partial x^2} - f_b = 0 \\ C_{11}^*\left(\dfrac{\partial^4 \phi}{\partial x^4} + \dfrac{1}{R^4}\dfrac{\partial^4 \phi}{\partial \theta^4}\right) + \dfrac{2}{R^2}(C_{66}^* + C_{12}^*)\dfrac{\partial^4 \phi}{\partial x^2 \partial \theta^2} + + \dfrac{1}{R}\dfrac{\partial^2 w}{\partial x^2} = 0 \end{cases}. \tag{10}$$

3. PROPERTIES OF POROUS FGM CYLINDRICAL SHELL

We consider that FGMs produced using ceramic and metal materials, we also suppose that the porosities are distributed in the area of the cross section of porous FGM shell. Using the modified rule of mixture [39], the Young's modulus E and Poisson's ratio ν of the porous FGM shell are expressed as follows:

$$\begin{cases} E(z) = E_m\left(V_m - \dfrac{\alpha}{2}\right) + E_c\left(V_c - \dfrac{\alpha}{2}\right) \\ \nu(z) = \nu_m\left(V_m - \dfrac{\alpha}{2}\right) + \nu_c\left(V_c - \dfrac{\alpha}{2}\right) \end{cases}, \tag{11}$$

where E_m and E_c are the Young's modulus of ceramic and metal, respectively. ν_m and ν_c are the Poisson's ratio of ceramic and metal, respectively, and $\alpha(0 \leq \alpha \ll 1)$ is the porosity volume fraction. V_m and V_c are volume fraction of ceramic and metal, respectively, they are expressed by:

$$\begin{cases} V_c(z) = \left(\dfrac{1}{2} + \dfrac{z}{h}\right)^n \\ V_m(z) = 1 - V_c(z) \end{cases}, \tag{12}$$

with the power-law index n of material varies in the interval $(0 \leq n \leq \infty)$.

4. BUCKLING BEHAVIOR OF POROUS FGM CYLINDRICAL SHELL RESTING ON ELASTIC FOUNDATION

We can solve directly the problem of the interaction between FGP cylindrical shell and an elastic foundation as an external medium. In the contact surface, the displacement at any point can be calculated as function of pressure throughout the zone contact, which causes the challenges of elastic contact stress theory. In this case we must find the solution of an integral equation for the pressure. When we cannot consider the external medium as an elastic material, we cannot write its behavior using the equations of elasticity, which leads to another problem. We can avoid the difficulties mentioned above if the response of the cylindrical shell is more interesting then the stresses distribution and displacements in the external medium. We can avoid the difficulties mentioned above if we are very interested by the response of the cylindrical shell then the stresses distribution and displacements in the external medium. So the effect of the external medium on the lateral surface of the shell can be expressed by a relatively simple foundation models using the shell displacements. Various foundations models are collected in [40-43]. The design of these models is based on the replacement of an external medium by springs coupled with dissipative elements. If we consider that there are just springs and taking into account their shear interactions, the relationship between contact pressure and porous FGM cylindrical shell can be expressed, according to the foundation deflection, as follows:

$$\begin{cases} f = K_W w \qquad for\ the\ Winkler\ model \\ f = K_W w - K_G \nabla^2 w \qquad for\ the\ Pasterrnak\ model \\ f = \frac{1}{1+\frac{K_W}{K_C}}\left(K_W w - K_G \nabla^2 w - \frac{DK_G}{K_C}\nabla^6 w\right) \qquad for\ the\ Kerr\ model \end{cases}, \tag{13}$$

where K_W is the Winkler modulus of lower spring, K_C is the Kerr modulus of upper spring, K_G is the Pasternak modulus of the intermediate shear layer. For the Winkler model the reaction force of FGP cylindrical shell, at each point in the foundation, is given in terms of the foundation deflection, which amounts to modeling the foundation by a juxtaposition of elastic springs [42]. The Pasternak model assumes that there is a shear interaction between the springs [43]. In the Kerr model, another parameter has been added for the enrichment of the foundation model [41], where the surrounding elastic medium is envisaged to be a sandwich material consisting of lower and upper spring beds and a shear layer in the middle (see Figure 1-(b)), this gives more flexibility for the continuity of the foundation between unloaded and loaded area of porous FGM cylindrical shell.

Using the systems (10) and (13), the displacement $w(x,\theta)$ in the transverse direction and the stress functions $\phi(x,\theta)$ are solutions of the equilibrium problem given by the two equations below:

$$\begin{cases} -D\left(\frac{\partial^4 w_b}{\partial x^4} + \frac{2}{R^2}\frac{\partial^4 w_b}{\partial x^2 \partial \theta^2} + \frac{1}{R^4}\frac{\partial^4 w_b}{\partial \theta^4}\right) + \frac{1}{R}\frac{\partial^2 \phi}{\partial x^2} + \lambda \frac{\partial^2 w_b}{\partial x^2} - \frac{1}{1+\frac{K_W}{K_C}}\left(K_W w - K_G \nabla^2 w - \frac{DK_G}{K_C}\nabla^6 w\right) = 0 \\ C_{11}^*\left(\frac{\partial^4 \phi}{\partial x^4} + \frac{1}{R^4}\frac{\partial^4 \phi}{\partial \theta^4}\right) + \frac{2}{R^2}(C_{66}^* + C_{12}^*)\frac{\partial^4 \phi}{\partial x^2 \partial \theta^2} + + \frac{1}{R}\frac{\partial^2 w}{\partial x^2} = 0 \end{cases} \tag{14}$$

,

One can express the solution of the problem (14) as follows:

$$\begin{cases} w(x,\theta) = Ae^{\left(i\frac{m\pi}{L}x\right)}\cos(n\theta) \\ \phi(x,\theta) = ae^{\left(i\frac{m\pi}{L}x\right)}\cos(n\theta) \end{cases}. \tag{15}$$

where A and a are arbitrary constants, n is the circumferential half wavenumbers of porous FGM cylindrical shell and m is its axial half wavenumbers. The substitution of the solution (15) in the problem (14) leads to:

$$\begin{cases} -D(\mathrm{p}^4 + 2\mathrm{p}^2\mathrm{q}^2 + \mathrm{q}^4)\mathrm{A} - \rho\mathrm{p}^2\mathrm{a} + \lambda\mathrm{p}^2\mathrm{A} \\ -\frac{1}{1+\frac{K_W}{K_C}}\left(K_W - K_G(\mathrm{p}^2+\mathrm{q}^2) + \frac{DK_G}{K_C}(p^6 + 3\mathrm{p}^4\mathrm{q}^2 + 3\mathrm{p}^2\mathrm{q}^4 + \mathrm{q}^6)\right)A = 0, \\ C_{11}^*(\mathrm{p}^4 + \mathrm{q}^4)\mathrm{a} + 2(C_{66}^* + C_{12}^*)\mathrm{p}^2\mathrm{q}^2\mathrm{a} - \frac{1}{R}\mathrm{p}^2 A = 0 \end{cases} \tag{16}$$

where $\rho = 1/\mathrm{R}$ is the curvature and $\mathrm{p} = \mathrm{m}\pi/\mathrm{L}$ and $\mathrm{q} = \mathrm{n}/\mathrm{R}$ are the wave numbers in axial and circumferential direction, respectively. The second equation of the system (16) leads to determine the constant a:

$$\mathrm{a} = \frac{\rho\mathrm{p}^2\mathrm{A}}{C_{11}^*(\mathrm{p}^4+\mathrm{q}^4)+2(C_{66}^*+C_{12}^*)\mathrm{p}^2\mathrm{q}^2}. \tag{17}$$

Using the value of "a", the first equation of the system (16) can be writtenin the following form:

$$-D(1+2\beta^2+\beta^4)\mathrm{p}^4-\frac{\rho^2}{C_{11}^*(1+\beta^4)+2(C_{66}^*+C_{12}^*)\beta^2}+\lambda\mathrm{p}^2-\frac{1}{1+\frac{K_W}{K_C}}\Big(K_W+K_G(1+\beta^2)\mathrm{p}^2+\frac{DK_G}{K_C}(1+3\beta^2+3\beta^4+\beta^6)\mathrm{p}^6\Big)=0, \tag{18}$$

where $\beta=\mathrm{q}/\mathrm{p}$ is the aspect ratio. So, we can determine the expression of the buckling load λ as a function of two variables β and p as follows:

$$\lambda(\beta,p)=D(1+2\beta^2+\beta^4)\mathrm{p}^2+\left(\frac{\rho^2}{C_{11}^*(1+\beta^4)+2(C_{66}^*+C_{12}^*)\beta^2}+\frac{K_W}{1+\frac{K_W}{K_C}}\right)\frac{1}{\mathrm{p}^2}+\frac{K_G(1+\beta^2)}{1+\frac{K_W}{K_C}}+\frac{\frac{DK_G}{K_C}(1+3\beta^2+3\beta^4+\beta^6)}{1+\frac{K_W}{K_C}}\mathrm{p}^4. \tag{19}$$

The minimization of the buckling load $\lambda(\beta,p)$ in Equation (19) compared to " p" allows us to determinate the critical buckling load λ_{cr} :

$$\left.\frac{\partial\lambda(\beta,p)}{\partial p}\right|_{\beta\text{ fixed}}=0, \tag{20}$$

This minimization gives the polynomial (21) of degree 6 in p

$$D(1+2\beta^2+\beta^4)\mathrm{p}^4-\left(\frac{\rho^2}{C_{11}^*(1+\beta^4)+2(C_{66}^*+C_{12}^*)\beta^2}+\frac{K_W}{1+\frac{K_W}{K_C}}\right)+2\frac{\frac{DK_G}{K_C}(1+3\beta^2+3\beta^4+\beta^6)}{1+\frac{K_W}{K_C}}\mathrm{p}^6=0. \tag{21}$$

By putting $\Lambda=\mathrm{p}^2$, we can reduce the degree of the polynomial and rewrite Equation (21) as follows:

$$b_1\Lambda^3+b_2\Lambda^2+b_3=0, \tag{22}$$

where

$$\begin{cases} b_1=2\dfrac{\frac{DK_G}{K_C}(1+3\beta^2+3\beta^4+\beta^6)}{1+\frac{K_W}{K_C}} \\ b_2=D(1+2\beta^2+\beta^4) \\ b_3=-\left(\dfrac{\rho^2}{C_{11}^*(1+\beta^4)+2(C_{66}^*+C_{12}^*)\beta^2}+\dfrac{K_W}{1+\frac{K_W}{K_C}}\right) \end{cases}, \tag{23}$$

If we divide by "b_1" and we put $\Lambda=\mathrm{X}-\frac{b_2}{3b_1}$, it is then reduced to the form:

$$\mathrm{X}^3+d_1\mathrm{X}+d_2=0, \tag{24}$$

with $d_1=-\frac{\mathrm{b}_2^2}{3\mathrm{b}_1^2}$ and $d_2=\frac{2\mathrm{b}_2^3}{27\mathrm{b}_1^3}+\frac{\mathrm{b}_3}{\mathrm{b}_1}$. The only real root of Equation (29) is given by:

$$\mathrm{X}=\sqrt[3]{-\frac{\mathrm{d}_2}{2}+\sqrt{\frac{\mathrm{d}_2^2}{4}+\frac{\mathrm{d}_1^3}{27}}}+\sqrt[3]{-\frac{\mathrm{d}_2}{2}-\sqrt{\frac{\mathrm{d}_2^2}{4}+\frac{\mathrm{d}_1^3}{27}}}, \tag{25}$$

So we can conclude the critical axial wave number $\mathrm{p_{cr}}$ which is equal:

$$\mathrm{p_{cr}} = \left(\mathrm{X} - \frac{\mathrm{b_2}}{3\mathrm{b_1}}\right)^{\frac{1}{2}}. \tag{26}$$

We can simplify the expression of buckling load for the Porous FGM cylindrical shell resting on Winkler or Pasternak elastic mediums as follows:

$$\lambda(\beta, p) = D(\,1 + 2\beta^2 + \beta^4)\mathrm{p}^2 + \left(\frac{\rho^2}{C_{11}^*(1+\beta^4)+2(C_{66}^*+C_{12}^*)\beta^2} + K_W\right)\frac{1}{\mathrm{p}^2} + K_G(1+\beta^2). \tag{27}$$

By minimizing this buckling load $\lambda(\beta, p)$ compared to "p", we obtain a polynomial of degree 4 in "p":

$$D(\,1 + 2\beta^2 + \beta^4)\mathrm{p}^4 - \left(\frac{\rho^2}{C_{11}^*(1+\beta^4)+2(C_{66}^*+C_{12}^*)\beta^2} + K_W\right) = 0. \tag{28}$$

Equation (28) leads to the critical axial wave number pcr which is equal:

$$p_{cr} = \left(\frac{\frac{\rho^2}{C_{11}^*(1+\beta^4)+2(C_{66}^*+C_{12}^*)\beta^2}+K_W}{D(\,1+2\beta^2+\beta^4)}\right)^{\frac{1}{4}}. \tag{29}$$

Finally we can obtained the critical buckling load of porous FGM cylindrical shell resting on an elastic medium, according to the critical axial wave number p_{cr}, as follows $\lambda_{cr} = \lambda(p = p_{cr})$.

5. NUMERICAL ANALYSIS

In this section of the numerical analysis, some studies of the buckling of porous FGM cylindrical shell subjected to an axial compression are presented. We consider that the porous FGM shell is made of steel (ceramic) and aluminum (metal). The geometrical and material properties are: the inner diameter $R = 100mm$, the thickness $H = 10mm$, the length $L = 10R$, the Young's moduli $E_c = 207GPa$ and $E_m = 69GPa$, the Poison's ratio $\nu = 0.3$. The porosity volume fraction α is defined in the range of $0 \leq \alpha \ll 1$ and the power-law index n in the range of $0 \leq n \ll 1$. In the buckling analysis of porous FGM cylindrical shell presented in this work, we compute the results by a dimensionless form of the critical buckling load parameter as:

$$\bar{\lambda}_{cr} = \frac{\lambda_{\mathrm{cr}}}{\mathrm{C_{110}}}, \tag{30}$$

and also by dimensionless forms of the Winkler, Pasternak and Kerr constants as:

$$\begin{cases} \beta_W = \frac{K_W \mathrm{L}^2}{\mathrm{C_{110}}} \\ \beta_G = \frac{K_G}{\mathrm{C_{110}}} \\ \beta_C = \frac{K_C \mathrm{L}^2}{\mathrm{C_{110}}} \end{cases}, \tag{31}$$

where $\mathrm{C_{110}}$ is the extension stiffness of the ceramic material only given by:

$$\mathrm{C_{110}} = \int_{-h/2}^{h/2}\left(\frac{E_C}{(1-\nu_C^2)}\right)dz. \tag{32}$$

In the analysis, we investigate the effect of power-law index, porosity volume fraction, and Young's modulus ratio ($M = E_m/E_c$).

5.1. Analysis of the Effect of Power-Law Index

In this study, five power-law indices ($n = 0, 1, 2, 3, 4, 5$) and two porosity volume fraction values ($\alpha = 0, 0.1$) are considered to examine the effect of power-law index n on the buckling behavior of a straight porous FGM cylindrical shell. Figures 2(a)-(b) explain the effect of the power-law index on critical buckling load versus the aspect ratio β for two porosity volume fraction values. From Figures (a)-(b), the increase of the power-law index n leads to the decrease of the critical buckling load of the porous FGM, which shows that the increase of n leads to the decrease of the porous FGM rigidity.

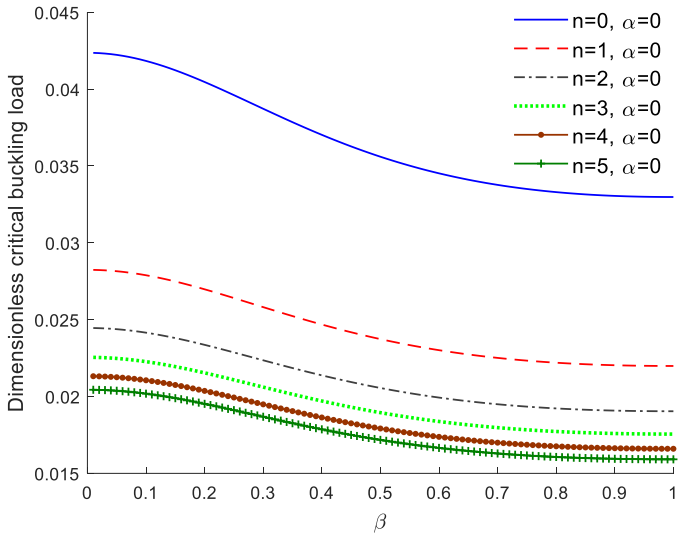

(a) : Dimensionless critical buckling load $\bar{\lambda}_{cr}$ versus aspect ratio β for $\alpha = 0$

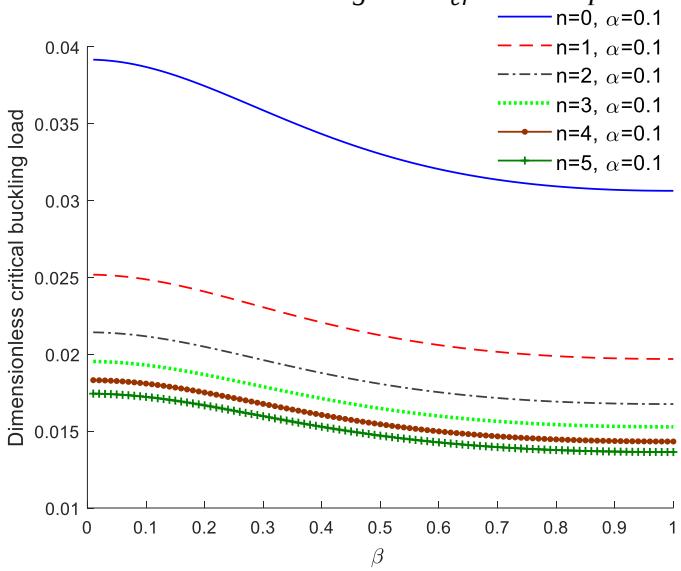

(b): Dimensionless critical buckling load $\bar{\lambda}_{cr}$ versus aspect ratio β for $\alpha = 0.1$

Figure 2. *Analysis of the effect of power-law index n on the critical buckling load of porous FGM shell with two porosity volume fraction values $\alpha = 0$ and 0.1*

5.2. Analysis of the Effect of Porosity Volume Fraction (α)

The analysis of the effect of porosity volume fraction α on the critical buckling load of porous FGM shell is presented in Figures 3(a)-(b). Two power-law index values ($n = 0, 1$) are considered. We observe from Figures 3(a)-(b) that $\bar{\lambda}_{cr}$ is affected considerably by the porosity volume fraction α. When the value of power-law index n is fixed, the results indicate that the increase in the porosity volume fraction α leads to

the decrease of critical buckling loads. This behavior shows that the porosity distribution affect the stiffness of the porous FGM shell.

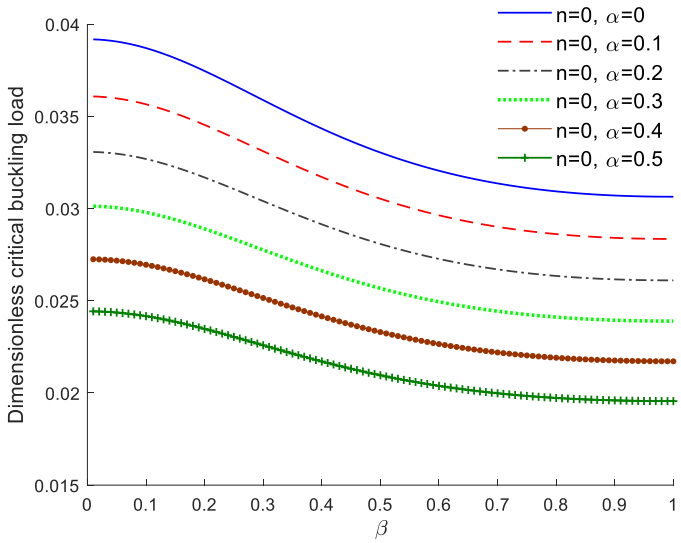

(a) : Dimensionless critical buckling load $\bar{\lambda}_{cr}$ versus aspect ratio β for $n = 0$

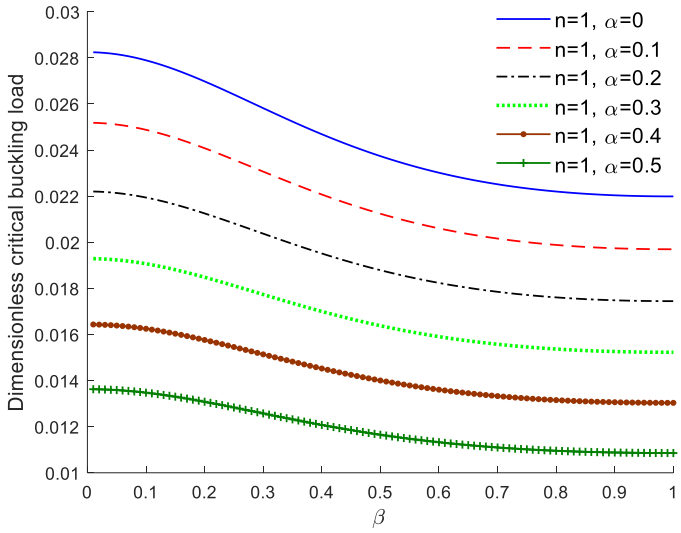

(b): Dimensionless critical buckling load $\bar{\lambda}_{cr}$ versus aspect ratio β for $n = 1$

Figure 3. *Analysis of the effect of porosity volume fraction α on the critical buckling load of porous FGM shell with two power law indices values $n = 0$ and 1*

5.3. Analysis of the Effect of Young's Modulus Ratio (*M*)

In this study, five Young's modulus ratio values ($n = 0.25, 0.5, 1, 5, 10$) and the aspect ratio $\beta = 0.6$ are considered. In Table 1 we present the dimensionless critical buckling with several values of Young's modulus ratio (M). We can observe in this table that $\bar{\lambda}_{cr}$ increases with increasing M for a constant value of n. Moreover, if the power-law index increases, we can notice that the critical buckling load decreases if $M < 1$, increases if $M > 1$ and it is not affected when $M = 1$.

Table 1. *Dimensionless critical buckling load $\bar{\lambda}_{cr}$ of porous FGM cylindrical shell*

A	M	n				
		2	4	6	8	10
0.0	0.25	0.0181	0.0152	0.0138	0.0129	0.0123
	0.5	0.0236	0.0217	0.0207	0.0201	0.0197

	1	0.0345	0.0345	0.0345	0.0345	0.0345
	5	0.1219	0.1369	0.1444	0.1493	0.1526
	10	0.2311	0.2647	0.2817	0.2926	0.3002
0.1	0.25	0.0159	0.0130	0.0115	0.0107	0.0100
	0.5	0.0209	0.0190	0.0180	0.0174	0.0170
	1	0.0309	0.0309	0.0309	0.0309	0.0309
	5	0.1109	0.1258	0.1333	0.1381	0.1415
	10	0.2109	0.2444	0.2613	0.2721	0.2797
0.4	0.25	0.0093	0.0064	0.0049	0.0040	0.0034
	0.5	0.0130	0.0111	0.0102	0.0096	0.0092
	1	0.0204	0.0204	0.0204	0.0204	0.0204
	5	0.0792	0.0939	0.1014	0.1061	0.1095
	10	0.1527	0.1857	0.2025	0.2133	0.2208

5.4. Analysis of the Effect of Elastic Foundation Parameters

To analyze the potential impact of the elastic medium parameters on the buckling response of the porous FGM cylindrical shell, we consider the aspect ratio $\beta = 0.6$ and we study three different types of foundations which are given as follows $(\beta_W = 5, \beta_G = 0, \beta_C = 0)$, $(\beta_W = 5, \beta_G = 0.5, \beta_C = 0)$ and $(\beta_W = 5, \beta_G = 0.5, \beta_C = 1)$. Table 2 explains the effect of elastic foundation parameters on the dimensionless critical buckling load of the porous FGM cylindrical shell. We can see in Table 2 that by varying the porosity volume fraction for a fixed value of the power-law index, the porous FGM shell exhibits large deformation with a small porosity volume fraction, the same remark can be observed by varying the power-law index with a fixed value of the porosity volume fraction. These remarks remain valid for the three types of foundations.

Table 2. *Effects of porosity on buckling of porous FGM shell with different foundation parameters*

$(\beta_W, \beta_G, \beta_C)$	α	n		
		2	6	10
Winkler foundation $(5, 0, 0)$	0	0.0232	0.0195	0.0181
	0.1	0.0208	0.0171	0.0157
	0.4	0.0136	0.0099	0.0085
Pasternak foundation $(5, 0.5, 0)$	0	0.7032	0.6995	0.6981
	0.1	0.7008	0.6971	0.6957
	0.4	0.6936	0.6899	0.6885
Kerr foundation $(5, 0.5, 1)$	0	0.2208	0.1998	0.1930
	0.1	0.2086	0.1876	0.1808
	0.4	0.1723	0.1512	0.1444

For Kerr elastic medium, we conclude from Figure 4 that $\bar{\lambda}_{cr}$ decreases most rapidly with the increase of the porosity volume fraction α compared to Winkler and Pasternak elastic mediums.

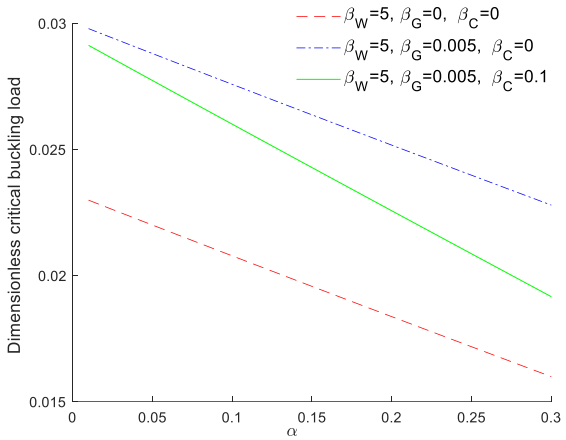

Figure 4. *Effects of porosity on buckling with different foundation parameters ($n = 2$)*

Variation of critical buckling loads with dimensionless Winkler and Pasternak parameter is depicted in Figure 5. It can be observed from the figure that the effect of the Pasternak foundation parameter is more significant for porous FGM cylindrical shell than the Winkler foundation parameter.

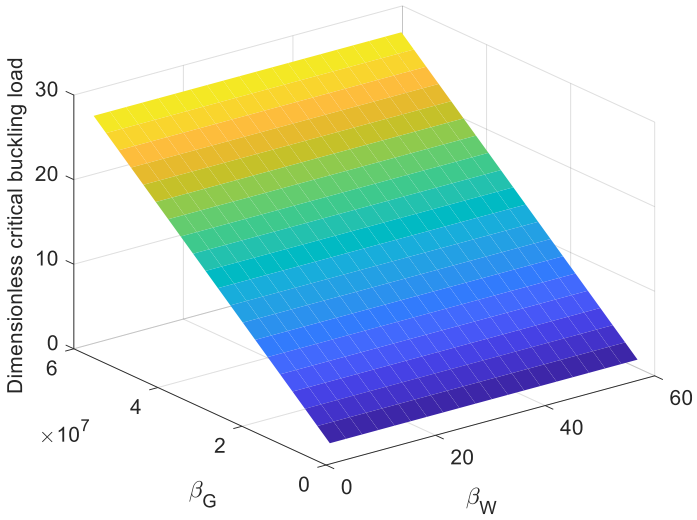

Figure 5. *The variation of critical buckling loads with nondimensional foundation parameters ($n = 2, \alpha = 0.1$)*

As shown in Figure 6, we observe that the Winkler medium makes the porous FGM shell less rigid compared to the Pasternak medium. But the comparison between Kerr and others mediums depends on the value of β_C, where for great values of β_C the Kerr model tends to that of Pasternak.

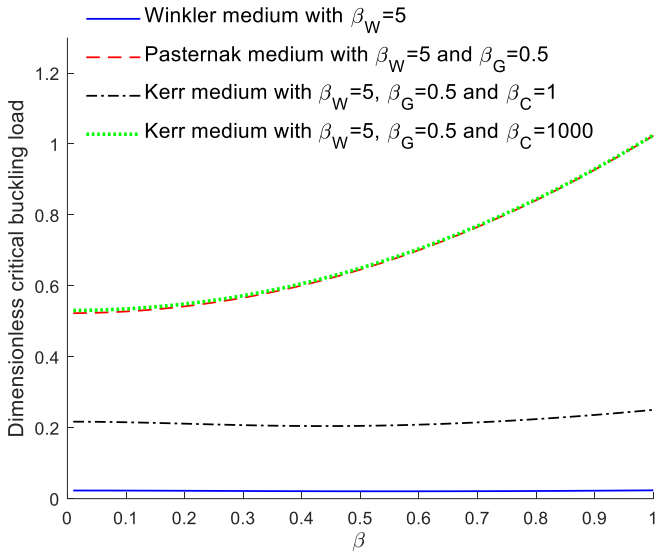

Figure 6. *Dimensionless critical buckling load $\bar{\lambda}_{cr}$ of porous FGM shell versus aspect ratio β for the three foundations models*

The influence of the elastic matrix on $\bar{\lambda}_{cr}$ is illustrated in Figure 7. This figure shows $\bar{\lambda}_{cr}$ versus moduli of elastic foundations. It is very clear that $\bar{\lambda}_{cr}$ rises most rapidly with the increase of β_W and β_G for Winkler (see Figure 7-(a)) and Pasternak (see Figure 7-(b)) elastic mediums, respectively. In the case of Kerr medium (see Figure 7-(c)), $\bar{\lambda}_{cr}$ rises most quickly with the increase of β_C, if the value of β_C exceeds a certain value the increase of $\bar{\lambda}_{cr}$ slows gradually.

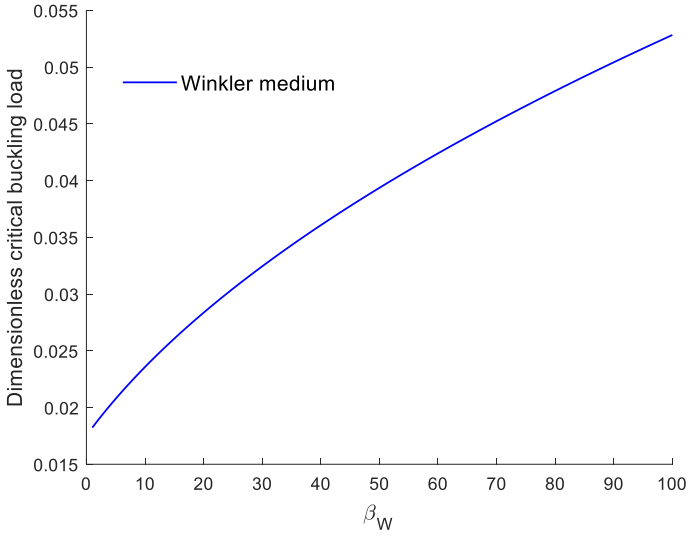

(a) : $\bar{\lambda}_{cr}$ versus β_W for the Winkler foundation model

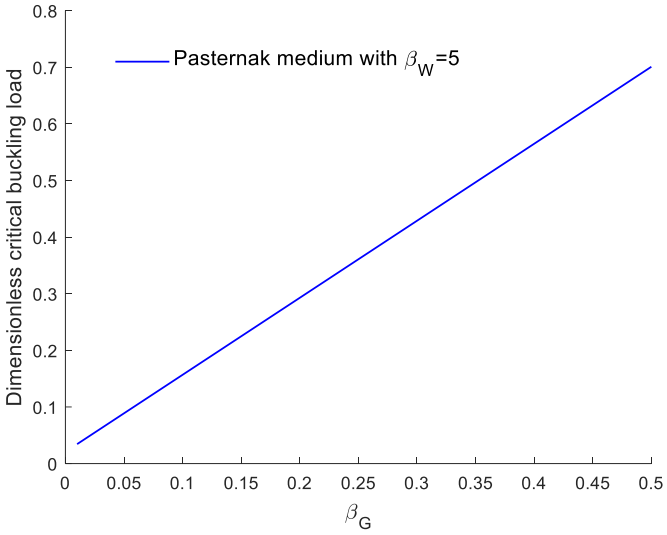

(b) : $\bar{\lambda}_{cr}$ versus β_G for the Pasternak foundation model

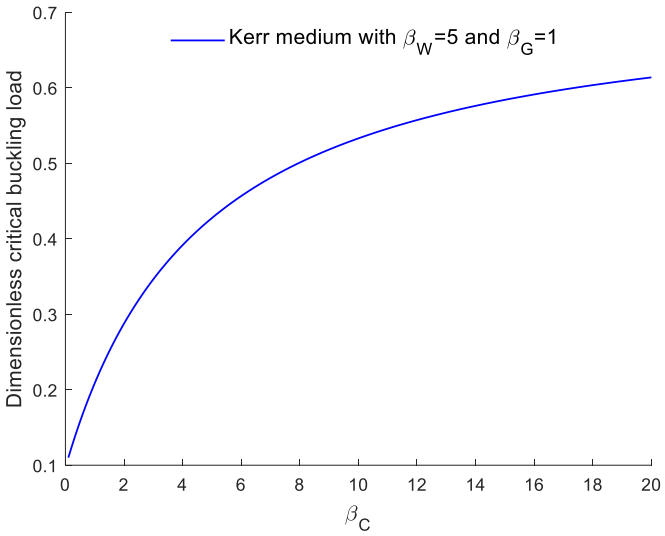

(c): $\bar{\lambda}_{cr}$ versus β_C for the Kerr foundation model

Figure 7. *Critical buckling load $\bar{\lambda}_{cr}$ of porous FGM shell versus the elastic foundation parameters*

6. CONCLUSION

In this article, buckling behaviors of porous FGM cylindrical shell resting on Winkler, Pasternak and Kerr foundations are investigated. The influences of power law index (n), porosity volume fraction (α), Young's modulus ratio (M) and elastic foundation parameters on buckling are explored. The following results are obtained:

- Critical buckling load values of porous FGM shell decrease with increasing power law exponent. Therefore, increasing the value of power law index makes the porous FGM shell less rigid.

- Increasing of the porosity volume fraction α results in a lower critical buckling load for porous FGM cylindrical shell. Therefore, the porous FGM shell becomes lighter when α increases, which explains that the porosity distribution effect must be taken into account in the study of porous FGM shells.

- The critical buckling load decreases with increasing the Young's modulus ratio and for a given value of Young's modulus ratio, as the power law index increases, the critical buckling load decreases for $M < 1$ and increases if $M > 1$. It is noticed that when M = 1, critical buckling load is note affected by the change of values of power law exponent.

- Winkler, Pasternak and Kerr foundation parameters increase the critical buckling loads of the porous FGM shell.

- Porous FGM cylindrical shell resting on Pasternak foundation has the highest critical buckling load values. The effect of the Pasternak foundation parameter is more significant for porous FGM shell than the Winkler foundation parameter.

- The effect of the power law exponent on the values of critical buckling loads reduces with the effect of elastic foundation.

- For great values of upper spring modulus the Kerr model tends to that of Pasternak.

- The power law exponent effects are more considerable for porous FGM shell resting on Kerr foundation.

Although this document deals with the analysis of buckling response, the extension of this study is also envisaged by considering the effects of spatial curvature of the geometry of shells, such as spherical shells, flat plates or other geometries as in the reference [44].

CONFLICTS OF INTEREST

No conflict of interest was declared by the author.

REFERENCES

[1] Mahamood, R. M., Akinlabi, E. T., "Types of functionally graded materials and their areas of application", Functionally Graded Materials, Springer, 5: 9-21, (2017).

[2] Bessaim, A., Houari, M. S. A., Tounsi, A., Mahmoud, S. R., Adda Bedia, E. A., "A new higher-order shear and normal deformation theory for the static and free vibration analysis of sandwich plates with functionally graded isotropic face sheets", Journal of Sandwich Structures and Materials, 15(6): 671-703, (2013).

[3] Tounsi, A., Houari, M. S. A., Benyoucef, S., Adda Bedia, E. A., "A refined trigonometric shear deformation theory for thermoelastic bending of functionally graded sandwich plates", Aerospace Science and Technology, 24(1): 209-220, (2013).

[4] Boggarapu, V., Gujjala, R., Ojha, S., Acharya, S., Venkateswara babu, P., Chowdary, S., kumar Gara, D., "State of the art in functionally graded materials", Composite Structures, 262: 113596, (2021).

[5] Bakhti, K., Kaci, A., Bousahla, A. A., Houari, M. S. A., Tounsi, A., Adda Bedia, E. A., "Large deformation analysis for functionally graded carbon nanotube-reinforced composite plates using an efficient and simple refined theory", Steel and Composite Structures, 14(4): 335-347, (2013).

[6] Banerjee, J. R., Ananthapuvirajah, A., "Free vibration of functionally graded beams and frameworks using the dynamic stiffness method", Journal of Sound and Vibration, 422: 34-47, (2018).

[7] Ould Larbi, L., Kaci, A., Houari, M. S. A., Tounsi, A., "An efficient shear deformation beam theory based on neutral surface position for bending and free vibration of functionally graded beams", Mechanics Based Design of Structures and Machines, 41(4): 421-433, (2013).

[8] Kou, K., Yang, Y., "A meshfree boundary-domain integral equation method for free vibration analysis of the functionally graded beams with open edged cracks", Composites Part B: Engineering, 156: 303-309, (2019).

[9] Mercan, K., Demir, C., Civalek, Ö., "Vibration analysis of FG cylindrical shells with power-law index using discrete singular convolution technique", Curved and Layered Structures, 3(1): 82-90, (2016).

[10] Dastjerdi, S., Akgöz, B., Civalek, Ö., "On the effect of viscoelasticity on behavior of gyroscopes", International Journal of Engineering Science, 149: 103236, (2020) .

[11] Naebe, M., Shirvanimoghaddam, K., "Functionally graded materials: A review of fabrication and properties", Applied Materials Today, 5: 223-245, (2016).

[12] Gong, J., Xuan, L., Ying, B., Wang, H., "Thermoelastic analysis of functionally graded porous materials with temperature-dependent properties by a staggered finite volume method", Composite Structures, 224: 111071, (2019).

[13] Keleshteri, M., Jelovica, J., "Nonlinear vibration behavior of functionally graded porous cylindrical panels", Composite Structures, 239: 112028, (2020).

[14] Kim, J., Zur, K.K., Reddy, J., "Bending, free vibration, and buckling of modified couples stress-based functionally graded porous micro-plates", Composite Structures, 209: 879-888, (2019).

[15] Chen, D., Yang, J., Kitipornchai, S., "Elastic buckling and static bending of shear deformable functionally graded porous beam", Composite Structures, 133: 54-61, (2015).

[16] Wang, Y., Wu, D., "Free vibration of functionally graded porous cylindrical shell using a sinusoidal shear deformation theory", Aerospace Science and Technology, 66: 83-91, (2017).

[17] Zhou, C., Wang, P., Li, W., "Fabrication of functionally graded porous polymer via supercritical co2 foaming", Composites Part B: Engineering, 42: 318-325, (2011).

[18] Fiorenzo A. F., "Generalized exponential, polynomial and trigonometric theories for vibration and stability analysis of porous FG sandwich beams resting on elastic foundations", Composites Part B: Engineering, 156: 303-309, (2019).

[19] Jalaei, M. H., Civalek, Ö., "on dynamic instability of magnetically embedded viscoelastic porous FG nanobeam", International Journal of Engineering Science, 143: 14-32, (2019).

[20] Ebrahimi, F., Zia, M., "Large amplitude nonlinear vibration analysis of functionally graded timoshenko beams with porosities", Acta Astronautica, 116: 117-125, (2015).

[21] Chen, D., Kitipornchai, S., Yang, J., "Nonlinear free vibration of shear deformable sandwich beam with a functionally graded porous core", Thin-Walled Structures, 107: 39-48, (2016).

[22] Atmane, H. A., Tounsi, A., Bernard, F., "Effect of thickness stretching and porosity on mechanical response of a functionally graded beams resting on elastic foundations", International Journal of Mechanics and Materials in Design, 13: 71-84, (2017).

[23] Berghouti, H., Adda Bedia, E.A., Benkhedda, A., Tounsi, A., "Vibration analysis of nonlocal porous nanobeams made of functionally graded material", Advances in Nano Research, 7(5): 351-364, (2019).

[24] Medani, M., Benahmed, A., Zidour, A., Heireche, H., Tounsi, A., Bousahla, A. A., Tounsi, A., Mahmoud, S. R., "Static and dynamic behavior of (FG-CNT) reinforced porous sandwich plate using energy principle", Steel and Composite Structures, 32: 595-610, (2019).

[25] Kaddari, M., Kaci, A., Bousahla, A. A., Tounsi, A., Bourada, F., Tounsi, A., Bedia, E. A. A., Al-Osta, M. A., "A study on the structural behaviour of functionally graded porous plates on elastic foundation using a new quasi-3D model: Bending and free vibration analysis", Computers and Concrete, 25(1): 37-57, (2020).

[26] Jena, S. K., Chakraverty, S., Malikan, M., "Application of shifted Chebyshev polynomial-based Rayleigh–Ritz method and Navier's technique for vibration analysis of a functionally graded porous beam embedded in Kerr foundation", Engineering with Computers, (2020). https://doi.org/10.1007/s00366-020-01018-7

[27] Tran, T. T., Pham, Q. H., Nguyen-Thoi, T., "An Edge-Based Smoothed Finite Element for Free Vibration Analysis of Functionally Graded Porous (FGP) Plates on Elastic Foundation Taking into Mass (EFTIM)", Mathematical Problems in Engineering, 2020: 1-17, (2020).

[28] Ebrahimi, F., Dabbagh, A., Rastgoo, A., "Vibration analysis of porous metal foam shells rested on an elastic substrate", The Journal of Strain Analysis for Engineering Design, 54(3): 199-208, (2019).

[29] Jouneghani, F. Z., Dimitri, R., Bacciocchi, M., Tornabene, F., "Free Vibration Analysis of Functionally Graded Porous Doubly-Curved Shells Based on the First-Order Shear Deformation Theory", Applied Science, 7(12): 1252, (2017).

[30] Wang, Y., Ye, C., Zu, J. W., "Identifying the temperature effect on the vibrations of functionally graded cylindrical shells with porosities", Applied Mathematics and Mechanics, 39: 1587-1604, (2018).

[31] Keddouri, A., Hadji, L., Tounsi, A., "Static analysis of functionally graded sandwich plates with porosities", Advances in materials Research, 8(3): 155-177, (2019).

[32] Donnell, L. H., "Stability of Thin-Walled Tubes Under Torsion", N.A.C.A. Technical Report No. 479, (1934).

[33] Timesli, A., "An efficient approach for prediction of the nonlocal critical buckling load of double-walled carbon nanotubes using the nonlocal Donnell shell theory", SN Applied Sciences, 2: 407, (2020).

[34] Timesli, A., "Prediction of the critical buckling load of SWCNT reinforced concrete cylindrical shell embedded in an elastic foundation", Computers and Concrete, 26(1): 53-62, (2020).

[35] Timesli, A., Braikat, B., Jamal, M., Damil, N., "Prediction of the critical buckling load of multi walled carbon nanotubes under axial compression", Comptes Rendus de l Académie des Sciences - Series IIB - Mechanics-Physics-Astronomy, 345(2): 158-168, (2017).

[36] Asghar, S., Naeem, M. N., Hussain, M., Taj, M., Tounsi, A., "Prediction and assessment of nonlocal natural frequencies of DWCNTs: Vibration analysis", Computers and Concrete, 25(2): 133-144, (2020).

[37] Erklig, A., Guzelbey, I. H., Cevik, A., "Finite element analysis of finite strain elastoplastic contact-impact problems", Gazi University Journal of Science, 23(3): 327 -338, (2010).

[38] Çelik, K., Kurt, E., Uzun, Y., "Experimental and theoretical explorations on the buckling piezoelectric layer under magnetic excitation", Journal of Electronic Materials, 46, 4003-4016, (2017).

[39] She, G. L., Yuan, F. G., Ren, Y. R., Liu, H. B., Xiao, W. S., "Nonlinear bending and vibration analysis of functionally graded porous tubes via a nonlocal strain gradient theory", Composite Structures, 203: 614-623, (2018).

[40] Kerr, A. D., "Elastic and viscoelastic foundation models", ASME, The Journal of Applied Mechanics, 31(3): 491-498, (1964).

[41] Kerr, A. D., "A study of a new foundation model", Acta Mechanica, 1: 135-147, (1965).

[42] Winkler, E., "Die Lehre von Elastizitat und Festigkeit (on Elasticity and Fixity)", Dominicus, Prague, (1867).

[43] Pasternak, P. L., "On a New Method of Analysis of an Elastic Foundation by Means of Two Foundation Constants", Gosudarstvennoe Izdatelstvo Literaturi po Stroitelstvu I Arkhitekture, Moscow, (1954).

[44] Çevik, M., "In-plane Vibration Analysis of Symmetric Angle-ply Laminated Composite Arches", Gazi University Journal of Science, 23(2): 187-199, (2010).